

Network-Accelerated Non-Contiguous Memory Transfers

Salvatore Di Girolamo^{1,4}, Konstantin Taranov¹, Andreas Kurth², Michael Schaffner², Timo Schneider¹, Jakub Beránek³, Maciej Besta¹, Luca Benini², Duncan Roweth⁴, Torsten Hoefler¹

¹Dept. of Computer Science, ETH Zürich, 8092 Zürich, Switzerland

²Integrated System Laboratory, ETH Zürich, 8092 Zürich, Switzerland

³IT4Innovations, VŠB - Technical University of Ostrava

⁴Cray UK Ltd.

¹{first.lastname}@inf.ethz.ch, ²{first.lastname}@iis.ee.ethz.ch, ³jakub.beranek@vsb.cz, ⁴{sdigirola, droweth}@cray.com

ABSTRACT

Applications often communicate data that is non-contiguous in the send- or the receive-buffer, e.g., when exchanging a column of a matrix stored in row-major order. While non-contiguous transfers are well supported in HPC (e.g., MPI derived datatypes), they can still be up to 5x slower than contiguous transfers of the same size. As we enter the era of network acceleration, we need to investigate which tasks to offload to the NIC: In this work we argue that non-contiguous memory transfers can be transparently network-accelerated, truly achieving zero-copy communications. We implement and extend sPIN, a packet streaming processor, within a Portals 4 NIC SST model, and evaluate strategies for NIC-offloaded processing of MPI datatypes, ranging from datatype-specific handlers to general solutions for any MPI datatype. We demonstrate up to 10x speedup in the unpack throughput of real applications, demonstrating that non-contiguous memory transfers are a first-class candidate for network acceleration.

1 MOTIVATION

The interconnect network is the most critical component of scalable HPC clusters. After decades of evolution of high-speed networking technologies, today's HPC networks are highly specialized. This evolution from early bus-based Ethernet created high-performance switches, OS-bypass, partially offloaded RDMA networks tuned to move data at hundreds of gigabits/s line-rate to the application's virtual memory space [1]. While all network-specific packet processing has been moved from the CPU into the Network Interface Card (NIC) by RDMA, some application-specific processing remains: e.g., sending and receiving CPUs may need to change the data layout or apply simple computations (e.g., filtering) to the communication data. Such data-centric transformations could be applied while the data is *on the move* through the NIC.

Programmable network acceleration is thus the next logical step to optimize the interaction between the network and the CPU. The simple observation that some functions could be efficiently executed on the NIC has led to various kinds of specialized and limited implementations by Mellanox [2], Cray [3], and Portals 4 [4–6]. However,

these acceleration systems can hardly be programmed by the application developer. Thus, the state of NIC acceleration is similar to the state of GPU acceleration in the early 2000's where complex shader languages had to be misused to accelerate computational tasks. To enable simple application-level network offload, Hoefler et al. introduced the streaming Processing in the Network (sPIN) concept that unifies an abstract machine and programming interface for network accelerators. As such, sPIN is similar to CUDA or OpenCL for compute accelerators and MPI or UPC for communication.

The sPIN programming model can express arbitrary packet processing tasks offloaded to the network card from user-level. Yet, not all tasks are amenable to offload and programmers must carefully select which pieces of applications to offload to the NIC. Network accelerated sPIN NICs are designed for data-movement-intensive workloads and cannot compete with compute accelerators, such as GPUs, for compute intensive tasks. The main potential of NIC acceleration arises when the data is transformed while it moves through the NIC. Here, we expect more efficient and faster data processing than on a CPU where data items move through deep memory hierarchies, most likely without any reuse. Thus, a careful selection of offloaded tasks is imperative for highest performance.

A class of operations that is amenable to NIC offload is the transfer of non-contiguous data, an important primitive in many scientific computing applications. For example, in a distributed graph traversal such as BFS, the algorithm sends data to all vertices that are neighbors of vertices in the current frontier on remote nodes—here both the source and the target data elements are scattered at different locations in memory depending on the graph structure. More regular applications, such as stencil computations in regular grids used in many PDE/ODE solvers communicate strided data at the boundaries. In applications, such as parallel Fast Fourier Transform, the network can even be used to transpose the matrix on the fly, without additional copies. Such non-contiguous data accesses can account for up to 90% of application communication overheads [7, 8] and optimizations can lead to speedups of up to 3.8x in practice [9].

Nearly all distributed memory programming and communication interfaces support the specification of non-contiguous data transfers. Those range from simple input/output vectors (iovecs) in the standard C library to recursive derived datatypes in the Message Passing Interface (MPI). With iovecs, programmers can specify a fixed number of arbitrary offsets in a message. While this is ideal for implementing communication protocols, the $O(m)$ overhead for messages of size m limits its utility. The second most common interface enables to specify strided (aka. vector) accesses, typically parameterized by three numbers: block size, stride, and count. Strided patterns are versatile but limited to fixed blocks arranged in a fixed stride.

Permission to make digital or hard copies of all or part of this work for personal or classroom use is granted without fee provided that copies are not made or distributed for profit or commercial advantage and that copies bear this notice and the full citation on the first page. Copyrights for components of this work owned by others than ACM must be honored. Abstracting with credit is permitted. To copy otherwise, or republish, to post on servers or to redistribute to lists, requires prior specific permission and/or a fee. Request permissions from permissions@acm.org.

SC '19, November 17–22, 2019, Denver, CO, USA

© 2019 Association for Computing Machinery.

ACM ISBN 978-1-4503-6229-0/19/11...\$15.00

<https://doi.org/10.1145/3295500.3356189>

The most comprehensive specification in MPI allows nested types, where a type can be used as a base-type for another constructor. This specification allows to express arbitrary data accesses with a single, concise representation [10].

In this work, we explore how to efficiently offload this most complete and complex specification to practical accelerated network cards. We study strategies for the implementation and acceleration of arbitrary derived datatypes. While many approaches exist for datatype acceleration (cf. [11–13]), it is not possible to transparently offload *arbitrary datatype processing* to network cards today and data is often received into a buffer and then copied (“unpacked”) by the CPU. We argue that full offload is a prerequisite for *true zero copy* communication, leading to significant benefits in performance and energy consumption. In short, our main contributions are:

- Design and implementation of *full* non-contiguous memory transfer processing on network accelerator architectures.
- We extend the existing sPIN interface with new scheduling strategies to accelerate datatypes processing.
- We show how sPIN-offloaded DDTs can improve the receiver consumption bandwidth.
- We prototype a sPIN hardware implementation that can be integrated into a NIC in a modern technology node.

2 BACKGROUND

Network-acceleration of memory transfers is a critical optimization to improve application communication phases. Remote Direct Memory Access (RDMA) plays a major role in this context, allowing the remote processes to perform read or write operations directly to/from the address space of the target processes.

Non-contiguous memory transfers move data that has to be copied to/from the target process memory according to a given (non-contiguous) data layout, making them more challenging to accelerate. A common solution to implement such transfers is to build input-output vectors of contiguous memory regions (i.e., memory offset, size), and offload them to the NIC. However, these vectors have to be built for each transfer (e.g., different addresses) and are not space efficient because they always require an overhead linear in the number of contiguous regions. In this work we show how next-generation network-acceleration engines, such as sPIN [14], can efficiently accelerate non-contiguous memory transfers. We now provide a brief overview of sPIN and discuss the importance of non-contiguous memory transfers in HPC.

2.1 Streaming Processing in the Network

sPIN is a programming model proposed by Hoefer et al.: it extends the RDMA and message matching concepts to enable the offloading of simple computing and data movement tasks to the NIC. Instead of processing full messages, sPIN lets the users specify simple kernels to be executed on a per-packet basis. The authors define a Portals 4 [4] extension to support sPIN, which we adopt in this paper.

2.1.1 Portals 4. Portals 4 is a network programming interface that supports one-sided Remote Direct Memory Access (RDMA) operations. With Portals 4, a process can expose parts of its memory over the network by specifying a list entry and appending it to the Portals 4 priority or overflow lists. The list entries appended to the

overflow list are used as fallback if no list entries are available in the priority list (e.g., for handling unexpected messages).

Portals 4 exposes a matching and a non-matching semantic. With the matching semantic, a list entry is said *matching list entry* (ME) and it is associated with a set of match bits. Whenever a node wants to issue a remote operation (e.g., put), it specifies the target node on which the operation has to be executed and the match bits: the operation will be executed on the area of memory described by a matched ME at the target (i.e., a ME with the same match bits). The operation is discarded if no matching MEs are found neither in the priority nor in the overflow list. The interface allows the matching phase and the operation itself to be executed directly on the NIC. If the non-matching semantic is used, the operation is executed on the first list entry available on the priority or overflow list.

Completion notifications (e.g., incoming operation executed, ack received) are signaled as lightweight counting events or full events posted on an event queue that can be accessed by the application.

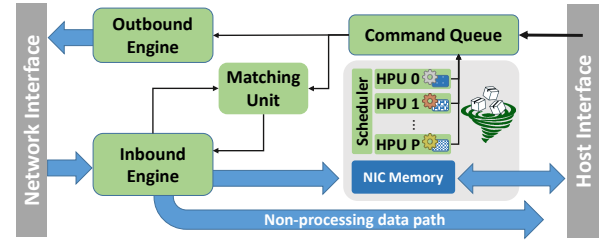


Figure 1: sPIN NIC Model

2.1.2 NIC Model. Fig. 1 shows a high level view of a NIC implementing sPIN. The message packets are delivered to the *inbound engine* which is responsible for parsing them and initiates the matching. There are three packet types: header (i.e., first packet of the message), completion (i.e., last packet), and payload (i.e., all the packets between the header and completion ones). The matching unit implements the Portals 4 priority and overflow lists: a message matches a memory descriptor (i.e., matching list entry or ME) if their match bits are equal. If the matching unit receives a matching request for a header packet, then the priority and the overflow list gets searched according to the Portals 4 matching semantic. After being matched, an ME can be unlinked from its list but is kept by the matching unit until the completion packet is received, so to match the rest of the message packets. We assume that the network delivers the header and the completion packets as the first and the last ones of a message, respectively.

2.1.3 Executing Handlers. A ME determines whether a packet has to be processed by sPIN. The set of handlers to be executed for the header, payload, and completion packets of a message, together with a NIC memory area that is shared by the handlers, is defined as *execution context*. The host application defines the execution context and associates it with an ME. If the matched ME is associated with an execution context, then the packet is copied in the NIC memory and a *Handler Execution Request* (HER) is sent to the scheduler, which will schedule the handler execution on a *Handler Processing Unit* (HPU). If the matched ME has no execution context associated with it, the data is copied to the host via the non-processing path. The packet gets discarded if no matching entries are found.

Fig. 2 shows the latency of a one-byte put operation (i.e., from when the data leaves the initiator to when it reaches the host memory). The data is collected from the simulation environment of Sec. 5. With sPIN, the latency is increased by $\sim 24\%$, that is the overhead for copying the packet to the NIC memory, scheduling the packet handler, and let it issue a DMA write command. While the latency depends on the complexity of the handlers, this data shows the minimum overhead introduced by sPIN.

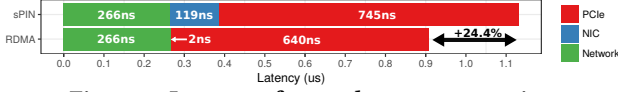


Figure 2: Latency of a one-byte put operation.

2.1.4 NIC Commands. The host can issue commands by pushing them to the NIC command queue (e.g., to instruct the *outbound engine* to send data). The HPUs can move data between the NIC and the host memory by issuing DMA write/read requests. The write requests can be *fire and forget* operations: the handler is not required to wait for transfer completion, allowing for a faster release of the HPU. The HPUs are also interfaced to the NIC command queue, allowing the handlers to start new communications (e.g., puts) by issuing NIC commands. The events (e.g., handlers or memory transfer completion, error states) are pushed to the event queue associated with the Portals 4 Table Entry to which the ME belongs.

2.2 Non-contiguous Memory Transfers

A key factor in the design of HPC applications is the memory layout they operate on. The decision of which layout to adopt is driven by many factors, such as readability of the code, the ability to vectorize, the ability to exploit locality and hardware prefetching.

As an example, the NAS LU [7, 15] uses a four-dimensional array as main data structure. This is split along two dimensions (x, y) onto a 2D processor grid. The first dimension contains 5 double-precision floats. Each (x, y)-plane corresponds to one iteration of the rhs-solver kernel. In each communication step, neighbouring faces (i.e., $n_x \times n_y \times 10$ elements) of the four-dimensional array are exchanged among processors, as sketched in Fig. 3.

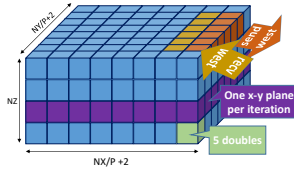


Figure 3: NAS LU data layout and communication.

Accelerating *Non-Contiguous Memory Transfers* (NCMT) is a common problem of HPC codes (e.g., the NAS LU benchmark exists since 1993), and (some) support for non-contiguous communications is present in all major HPC programming languages. When evaluating non-contiguous memory transfer support, an important consideration to make is the compactness of the resulting type map: Every non-contiguous memory transfer can be represented as a mapping from offsets in the source buffer to offsets in the destination buffer. The goal of NCMT-support is to exploit regularities in this mapping. ARMCI [16] for example supports two modes to transfer data, either using a list of source/destination pointers and a block size per pointer, or strided transfers (multiple stride levels are allowed). SHMEM [17] falls into the same category, however, strides cannot have multiple levels, thus sending a 3D array slice

can require multiple calls. Modern HPC languages such as CAF [18], UPC [19], Chapel and X10 support array slicing within the language and allow to assign slices to remote arrays but do not support transfers based on index lists directly (such support might not be needed if the compiler can aggregate multiple small sends at runtime).

In this paper we chose to focus on MPI [20] Derived Datatypes, which allow to specify strided, as well as index-list based transfers and allows arbitrarily deep nesting of type map descriptions. This decision was made because MPI supports the widest variety of type constructors, the NCMT support in any other of the mentioned languages/APIs can be easily mapped to MPI Derived Datatypes.

2.2.1 MPI Derived Datatypes. The simplest MPI Derived Datatypes (DDTs) directly map to the basic types of the languages interfaced with MPI, e.g., MPI_INT maps to an int in C. We call these predefined DDTs *elementary types*. In MPI, an integer stored in a variable v can be sent with MPI_Send(& v , 1, MPI_INT, ...). Now, if we need to send N contiguous integers we can either change the *count* argument in the MPI_Send call or construct a new DDT which describes this contiguous data-layout, using MPI_Type_contiguous(N , MPI_INT, &newtype), and supply newtype as the type of the MPI_Send(), setting *count* to 1.

To send blocks of data with a regular stride, e.g., a column of an N by N matrix (stored in row-major layout) we can construct an appropriate DDT using MPI_Type_vector(N , 1, N , MPI_INT, &newtype). The arguments specify the *count*, *block-length*, *stride*, *basetype*, *newtype*. If the data we need to communicate consists of a mix of types, i.e., an array of structs, we can use MPI_Type_create_struct(count, blocklens, displs, types, newtype) to construct an MPI DDT that maps to one element of the array, where count refers to the number of elements of the struct, displs gives the displacement for each struct entry in bytes (relative to the address of the struct itself), types is an array of MPI DDTs, one entry for each struct member. If the data we want to send is irregularly strided, we can use the MPI_Type_create_indexed_block(count, blocklength, displs, basetype, newtype) type constructor, which allows to pass a list of displacements and length per block. MPI supports additional type constructors not discussed here (e.g., MPI_Type_create_subarray()). Some DDT constructor calls described above support variants to, e.g., specify the displacements in bytes instead of multiples of *basetype*.

All MPI DDTs need to be *committed* before they can be used in any communication call. An MPI implementation which aims to optimize the implementation of DDTs can intercept the commit call to e.g., runtime-compile DDTs or prepare for their network offload.

Data can be locally packed and unpacked outside the communication functions with the MPI_Pack() and MPI_Unpack() calls, respectively. However, in doing so we forgo all possible optimizations MPI could perform, such as zero-copy data transfer, pipelining packing/sending, etc. The same is true for codes which perform “manual packing” of data before sending, a practice widespread in old HPC codes, due to the fact that a compiler can optimize the packing loops of specialized codes, e.g., utilize vector instructions to copy blocks, while a simple MPI implementation might only provide a non-specialized generic DDT interpreter. However, much effort has been directed into optimizing MPI DDT implementations, and using them often gives superior performance [21–23].

3 ACCELERATING NON-CONTIGUOUS MEMORY TRANSFERS

Fig. 4 sketches three possible implementations of non-contiguous memory transfers. The sender and receiver side implementations can be interchanged creating different solutions. The left tile shows the non-accelerated case: the sender CPU packs the data in a contiguous buffer before sending it and the receiver CPU unpacks it after receiving it. While this approach is efficient for small message sizes, the packing and unpacking overheads can limit the transfer performance of large messages. In the middle tile, the sender avoids the packing phase by streaming contiguous regions of data as they are identified. The receiver processes the incoming packets directly with sPIN: for each packet, a handler identifies one or more contiguous regions where the payload has to be copied to. However, the sender CPU is still busy finding the contiguous regions. This phase can be fully overlapped if we put sPIN on the NIC outbound path (right tile): the put-activated handlers can take care of the sender datatype processing and the issuing of the data transfers.

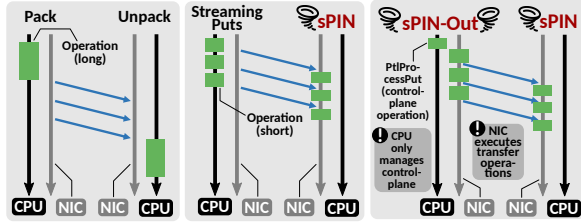


Figure 4: Network-accelerated DDT processing strategies.

3.1 Sending Non-Contiguous Data

In this section we outline the different strategies to accelerate datatype processing at the sender side.

3.1.1 Streaming Puts. The packing phase can be optimized by sending contiguous regions of data as they are identified, overlapping this communication with the search of the next region. Practically, this means splitting the send of the packed data in multiple put operations. However, the data sent by these multiple puts need to be seen as a single message by the receiver to, i.e., allow sPIN enforcing schedule dependencies and minimize the resource usage (e.g., events, match list entries).

We extend the Portals 4 interface introducing *streaming puts*, that allow to specify the message data via multiple function calls. A streaming put is started with a `Pt1SPutStart` call, which is similar to a `Pt1Put` but takes an additional parameter that is the contiguous memory descriptor $\langle \text{offset}, \text{size} \rangle$ identifying the data to be sent by this call. The applications can keep sending data as part of the same put operation by using `Pt1SPutStream` calls, that take as arguments: the streaming put descriptor, a contiguous memory region descriptor, and an *end-of-message* flag to specify if this call concludes the put operation. While Portals 4 already allows the same ME to be matched by different puts, these are seen as different messages, each of them triggering the message matching process, being processed as different messages by sPIN, and generating different events. A streaming put is transparent to the target since the packets generated by the different streaming put calls are part of the same message.

3.1.2 Outbound sPIN. Streaming puts improve the sender-side datatype processing performance but still require the sender CPU to be involved in the process. Full offloading of the sender-side datatype processing can be achieved by extending sPIN with the ability to process also packets that are being sent out. The idea is to have a new type of put operation (namely `Pt1ProcessPut`) that signals the NIC to create the packets of the message but, instead of injecting them on the network, forward them to the internal packet processing unit. In particular, the outbound engine creates a Handler Execution Request for each packet and sends it to the packet scheduler (as it happens for the incoming packets). In this case, we do not have the urgency to buffer the packet data in NIC memory since this is already stored in the host memory: for a `Pt1ProcessPut`, the outbound engine does not fill the packet with data (i.e., by DMAing it from host memory) but delegates this task to the packet handler.

In this model, the sender specifies an execution context to associate with the `Pt1ProcessPut` operation. This put operation leads to the generation of the packets and, for each one of these, a handler is executed on the sender NIC. The handler is in charge to identify the contiguous area of memory that the packet needs to carry (similarly to receiver-side datatype processing, see Sec. 3.2) and send the data out using a streaming put.

3.2 Receiving Non-Contiguous Data

We now describe how incoming messages are processed in sPIN according to a given datatype. We first introduce *packet scheduling policies*, an extension to sPIN that enables the user to influence the handler scheduling on the HPUs for a given message, then we describe the sPIN execution context to process datatypes on the NIC. Finally, we discuss two different approaches to datatype processing: with specialized or general handlers.

3.2.1 Packet Scheduling Policies. The sPIN scheduler enforces happens-before dependencies on the handlers execution: i.e., for a given message, the header handler executes before any payload handler and the completion handler executes after all the payload handlers. Ready-to-execute handlers are assigned to idle HPUs.

We extend the sPIN execution context to let the user specify scheduling policies different than the default one and implement a blocked round-robin packet scheduling policy, namely *blocked-RR*. With *blocked-RR*, sequences of Δp consecutive packets are sequentially processed: no two HPUs can execute handlers on the packets of this sequence at the same time. To avoid keeping HPUs busy waiting for the next packet of a sequence, we introduce *virtual HPUs* (vHPUs). They now become our scheduling units: a sequence of packets is assigned to a vHPU, that is scheduled to run on a physical HPU. The vHPU is in charge to process the handlers of the packets in the assigned sequence: if there are no packets to execute, the vHPU yields the HPU and gets rescheduled whenever a new packet of that sequence arrives. Packets of the same sequence can be processed out-of-order by the vHPU. The number of vHPUs and Δp are parameters of the scheduling policy.

3.2.2 DDT-Processing Execution Context. To offload datatype processing we need to create an ME to receive the data and a sPIN execution context to process it. In particular, we need to (1) install the header, payload, and completion handlers; (2) allocate and initialize

the NIC memory needed for the datatype processing; and (3) define the packet scheduling policy associated with this execution context. We now describe the general structure of the handlers, deferring their detailed implementation, the NIC memory management, and the scheduling policy selection to the following sections.

- **Header handler.** For datatype processing we do not perform any operation in the header handler, hence this is not installed.
- **Payload handler.** The payload handler identifies all the contiguous regions in receiver memory that are contained in a packet. For each one of them, it issues DMA write requests towards the receiver memory. Blocking and non-blocking DMA write requests are defined in sPIN. We always use non-blocking calls (i.e., `PltHandlerDMAToHostNB`) because our payload handlers do not need to wait for transfers completion. We extend this call adding the option `NO_EVENT` that, when specified, avoids that the transfer completion generates an event on the host.
- **Completion handler.** The completion handler issues a final zero-byte `PltHandlerDMAToHostNB` without the `NO_EVENT` option, so to generate the transfer completion event and signal the host that all the data has been unpacked.

3.2.3 Specialized Payload Handlers. To process incoming packets and derive the destination memory offsets, the payload handler needs to be aware of the datatype describing the memory layout. This awareness can be achieved with datatype-specific handlers or with generic ones operating on a datatype description. We now describe a set of handlers that are specialized for MPI Derived Datatypes having as base types an elementary type (e.g., `MPI_INT`, `MPI_FLOAT`) or contiguous types of elementary types. It is worth noting that in some cases more complex (i.e., nested) datatypes can be transformed to simpler ones via datatype normalization [24], potentially making them compatible with the specialized handlers.

The MPI *vector* datatype identifies a non-contiguous memory region that is composed of a fixed *number of blocks*. Blocks are composed of a *number of elements* of a certain *base type* and start *stride* elements apart from the previous one. To offload this datatype processing to sPIN, the host allocates a `spin_vec_t` data structure in the NIC memory containing the parameters described above. The pseudocode of the vector-specialized payload handler is shown in Listing 1. To improve readability, we show a simplified version of the handler, that does not handle the corner case where the block size does not divide the packet payload size. The handler first determines the host address where the first block of the packet has to be written to, then it proceeds to copy all the blocks contained in the packet payload at the right offsets (i.e., every *stride* bytes).

```
int vector_payload_handler(handler_args_t *args){
    uint8_t *pkt_payload = args->pkt_payload_ptr;
    uint8_t *host_base_ptr = args->ME->host_address;
    spin_vec_t *ddt_descr = (spin_vec_t *) args->mem;
    uint32_t block_size = ddt_descr->block_size;
    uint32_t stride = ddt_descr->stride;
    uint32_t host_offset = (args->pkt_offset / block_size)*stride;
    uint8_t *host_address = host_base_ptr + host_offset;

    for all the blocks in the packet payload {
        DMA write (pkt_payload, block_size) to host_address
        pkt_payload += block_size; host_address += stride;
    }
    return PTL_SUCCESS; }
```

Listing 1: Vector-specialized payload handler pseudocode

Other datatypes. More irregular memory areas can be described with more complex datatypes. For example, the *index-block* datatype models fixed-size blocks of elements displaced at arbitrary offsets. The *index* and *struct* datatypes extend it allowing to model variable size, or size and base type, memory regions, respectively.

To process these datatypes in sPIN, we need to provide the handlers with additional information (e.g., list of offsets and block sizes). The host application is in charge to copy this information to the NIC memory. The datatype influences also the handler complexity: e.g., to find the correct offset and block size for a given packet (or portion of a packet) we use a modified binary search on these lists that have size linear in the number of non-contiguous regions.

3.2.4 General Payload Handlers. Having specialized handlers always guarantees the best performance, but it is impossible to provide them for any arbitrary derived datatype. While the users are free to write handlers for their own datatypes (e.g., similar to writing custom unpack function), this solution does not apply to the general case. In this section we discuss a set of approaches to transparently process any derived datatype in sPIN, without the need of ad-hoc handlers. Our general handlers are based on the *MPITypes* library [25], that enables partial processing of MPI datatypes outside MPI. We optimize the library for faster offloaded execution by removing MPI dependencies and exchanging memory copy instructions with DMA write requests.

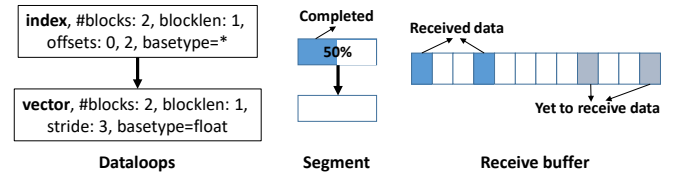


Figure 5: MPITypes dataloops for an index of vectors datatype; the segment representing the datatype processing state; and the receive buffer where the data is unpacked.

MPITypes. MPITypes library represents datatypes as sets of descriptors called *dataloops*. There are five types of dataloops: *contig*, *vector*, *blockindexed*, *indexed*, and *struct* [26]. Dataloops having elementary types as base type are defined as *leaves*. The processing of a datatype is split in two phases: (1) the non-leaf dataloops are traversed in order to determine the offset of the leaf, (2) the leaf datatype is processed to determine the relative offset in the receive buffer. Leaves are processed with specialized functions, similar to the specialized handlers of Sec. 3.2.3.

The partial progressing of datatypes is achieved by exporting the datatype processing state to a structure called *segment*. The state is represented by a stack, modeling the recursive processing of dataloops, and each element of the stack is a dataloop state. Fig. 5 shows an index of vectors datatype expressed with dataloops (left). The segment state (middle) shows that the index dataloop has already been progressed by 50%: i.e., one block (which is a vector datatype) has already been unpacked in the receive buffer (right).

The packed data is modeled as a stream of bytes: the datatype processing function takes a *first* and *last* bytes as input, representing the portion of stream to be processed (we always process one packet payload at a time). If the specified *first* byte is after the last byte processed in a given segment, a *catch-up* phase takes place:

the segment is progressed (without issuing DMA writes) until the position *first* is reached. Instead, if the *first* byte is before the last processed byte, then the segment is reset to its initial state.

The datatype processing function advances the state of the segment passed as input. In sPIN, multiple packets of the same message can be processed at the same time by different HPU, generating write conflicts if all of them use the same MPITypes segment. While a possible solution is to enforce mutual exclusion on the critical section inside MPITypes, this adds synchronization overheads that can serialize the handlers execution. We now discuss three approaches to datatype processing offload with MPITypes that avoid write-conflicts without requiring synchronization.

HPU-local. This strategy replicates the MPITypes segment on each vHPU, using blocked-RR as packet scheduling policy with $\Delta p = 1$ and the number of vHPUs P equal to the number of physical ones. While this solution completely removes the write-conflicts problem (i.e., each vHPU writes to its own segment), it is characterized by long catch-up phases during the datatype processing. In fact, assuming in-order packet arrival, each vHPU gets every other $P - 1$ packet: for each packet, it has to progress its state by $P - 1$ old packets (i.e., catch-up phase) before getting to the assigned one. In case of out-of-order packet delivery, a vHPU may receive a packet that is before the one processed last in its segment. In this case, the vHPU-local state is reset, incurring an additional overhead.

RO-CP: Read-Only Checkpoints. The idea of RO-CP is to solve the write-conflicts problem by avoiding the handlers to write back to shared memory. This is possible if each handler makes a local copy of the segment and then start processing on it, without writing the modified copy back. However, this would require each handler to always start the processing from the initial segment state. To address this issue, we introduce **checkpoints**: a checkpoint is a snapshot of the MPITypes segment processing state. Fig. 6 shows different checkpoints of the same segment: the datatype is processed on the host and every Δr bytes (we define Δr as checkpoint interval) a copy of the segment is made and used as checkpoint.

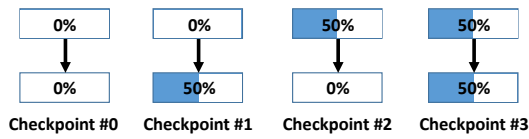


Figure 6: Checkpointing the segment state.

Whenever a handler executes on a packet, it selects the closest checkpoint that can be used to process the packet payload, makes a local copy of it, and then starts processing. This solution bounds the handler runtime to $O(\Delta r)$, but introduces the overhead of creating the checkpoints and copying them to the NIC. The checkpoint interval enables a tradeoff between the payload handler runtime and the NIC memory space needed to store the checkpoints: i.e., the smaller the checkpoint interval, the faster the handlers but also the more the checkpoints. For $\Delta r = k$, where k is the packet size, i.e., one checkpoint per packet: no catch-up phase and local segment copy are required (the checkpoint is used only once) but $\lceil \frac{m}{k} \rceil$ checkpoints are stored in NIC memory.

RW-CP: Progressing Checkpoints. The performance of the HPU-local and RO-CP is undermined by the long catch-up phase and the

checkpoint copy. We now discuss a solution that avoids the catch-up phase without requiring additional checkpoint copies in case of in-order packet arrival. The idea is to exploit the performance optimal case of RO-CP (i.e., $\Delta r = k$), assigning sequences of Δr consecutive packets to the each vHPU, that can now act as exclusive owners of a checkpoint. In this way we avoid the catch-up phase and the local copy even when $\Delta r > k$. This strategy can be implemented by using the blocked-RR scheduling policy (see Sec. 3.2.1) with $\Delta p = \lceil \frac{\Delta r}{k} \rceil$ and a number of vHPU equal to the number of packet sequences: all the packets using the same checkpoint get assigned to the same vHPU. In case of out-of-order packet delivery, the checkpoint state may be ahead of the received packet offset: in this case the changes to the checkpoint need to be reverted. We keep a master copy of the checkpoints in NIC memory, so they can be reset to their original checkpointed state if needed.

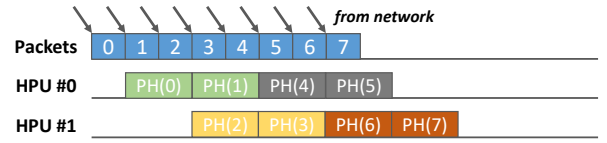


Figure 7: Packets scheduling in RW-CP ($\Delta r = 2 \cdot k$).

How do we select the checkpoint interval? While RW-CP optimizes the handler completion time, the employed blocked-RR scheduling policy introduces a packet scheduling dependency (i.e., the packets belonging to the same sequence cannot be processed in parallel, see Fig. 7), that influences the whole message processing time. We define message processing time as time from when the first byte of a message is received to when the last byte of the message is copied to the receiver buffer. We now model the message processing time for the RW-CP strategy, and discuss how to limit the scheduling overhead without overflowing the NIC memory.

Let us define the effective packet arrival time as T_{pkt} , the total number of packets composing a message of size m bytes as $n_{pkt} = \lceil \frac{m}{k} \rceil$, and P as the number of physical HPUs. We assume that $P < n_{pkt}$ for the sake of simplicity. The general payload handler runtime can be modeled as:

$$T_{PH}(\gamma) = T_{PH}^{init} + T_{PH}^{setup} + \gamma \cdot T_{PH}^{block}$$

where γ is the average number of contiguous memory blocks per packet, T_{PH}^{init} is the time needed to start the handler and prepare the arguments to pass to MPITypes (e.g., copy of the segment in RO-CP), T_{PH}^{setup} is the startup overhead of the datatype processing function (e.g., includes the catch-up phase), T_{PH}^{block} is the time needed by the datatype processing function to find the next contiguous block.

The message processing time of RW-CP can be modeled as:

$$T_C = T_{pkt} + \left\lceil \frac{\Delta r}{k} \right\rceil \cdot (P - 1) \cdot T_{pkt} + \left\lceil \frac{n_{pkt}}{P} \right\rceil \cdot T_{PH}(\gamma)$$

that is the time needed to receive/parse the first packet (T_{pkt}), plus the time to saturate the HPUs (we can schedule a new vHPU every $\lceil \frac{\Delta r}{k} \rceil$ received packets), plus the time taken by the last vHPU to process its share of packets (each vHPU gets $\lceil n_{pkt}/P \rceil$ packets).

The message processing time gets minimized for $\Delta r = 1$, but this requires to store a number of checkpoints equal to the number of packets. We observe that the overhead induced by Δr gets negligible

for large message sizes or for large values of γ . Hence, we can define a strategy to compute a checkpoint interval such that:

- The scheduling dependency overhead is less than a factor ϵ of the packets processing time:

$$T_{pkt} + \left\lceil \frac{\Delta r}{k} \right\rceil \cdot (P - 1) \cdot T_{pkt} \leq \epsilon \cdot \left\lceil \frac{n_{pkt}}{P} \right\rceil \cdot T_{PH}(\gamma)$$

- The total number of checkpoints fits in the NIC memory:

$$\frac{n_{pkt} \cdot k}{\Delta r} \cdot C \leq M_{NIC}$$

where C is the checkpoint size (612 B in our configuration).

- The packets buffered during the scheduling policy overhead fit in the packet buffer (B_{pkt} is the packet buffer size in bytes):

$$\min \left(\frac{T_{PH}(\gamma) \cdot k}{T_{pkt}}, \Delta r \right) \leq B_{pkt}$$

3.2.5 General vs. Specialized Payload Handlers. Fig. 8 shows the message processing throughput for a 4 MiB message with a vector datatype. We vary block size (x-axis) and stride (twice the blocksize). The benchmark reports the simulation results for an ARM-based (16 Cortex A15 HPUs @800MHz) sPIN implementation (see Sec. 5.1).

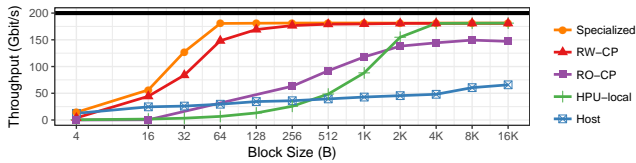


Figure 8: Unpacking throughput of an MPI_Type_vector as function of the block size.

The specialized handler reaches line rate already for 64 B block size (i.e., $\gamma = 32$). The throughput of RO-CP is limited by the segment copy, while the catch-up phase of HPU-local shrinks with the block size. The handlers become slower as the block size decreases (more iterations per handlers), making offloaded datatype processing slower than host-based unpack (i.e., RDMA + CPU unpack) for 4 B blocks.

3.2.6 Integration in MPI. Before starting to process a message with a given datatype, the host needs to configure the NIC to make it ready to execute the handlers as the packets arrive. In this section we discuss how to implement offloaded datatype processing in communication libraries, using MPI as driving example.

- (1) **Define the MPI derived datatype** and commit it. During the commit, the implementation determines the processing strategy to use (e.g., specialized or general handlers). according to the datatype being committed. At this stage, the DDT data structures to offload to the NIC are created: e.g., the checkpoints for the RO-CP and RW-CP.
- (2) **Post the receive operation.** During the posting of a receive using a derived datatype, the host tries to allocate NIC memory to store the DDT data structures. If the allocation fails due to the lack of space, the MPI implementation is free to (a) fall back to the non-offloaded DDT processing; or (b) free previously allocated memory (e.g., by applying a LRU policy on the offloaded datatypes). Once the NIC memory has been allocated and the DDT data structures copied to it, a ME is created and appended to the priority list.
- (3) **Complete the receive operation.** The MPI implementation gets an event whenever the datatype processing is over (i.e., all the DMA writes completed) and can conclude the receive.

The user can influence the NIC datatype processing by using the MPI_Type_set_attr call to specify the type attributes. Possible indications are: if the type has to be offloaded or not; the priority with which this type has to be offloaded (e.g., to drive the victim selection scheme if no NIC memory space is available during (2)); the ϵ parameter discussed in Sec.3.2.4.

Offloaded datatype processing is not possible for unexpected messages because the receiver-side datatype is not known at that stage (a matching receive has not been posted yet). They can be unpacked by falling back to the host CPU-based unpack methods.

4 PROTOTYPING SPIN

In this section, we propose a first design of a hardware implementation of sPIN, presenting first estimates for the complexity and power efficiency for a modern 22 nm technology implementation. Further, we validate the basic performance requirements in terms of throughput and memory bandwidth by running micro-benchmarks on a cycle-accurate simulation.

Design Goals and Requirements. The overall design goal is to fit the sPIN accelerator onto the same silicon die as the NIC, while ensuring that it is capable of sustaining a line rate of 200 Gbit/s. Hence the accelerator memory bandwidth must be matched, and the processing power must be aligned with the expected computational load. On typical DDT benchmarks we measured an average operational intensity (OI) around 0.04 - 0.08 op/B (w.r.t. the NIC input bandwidth), which turns into a load of 1-2 Gop/s at 200 Gbit/s. The use cases considered can allocate up to 3 MiB of temporary storage and hence a local memory with more than 6 MiB should be employed to enable efficient operation with double-buffering.

4.1 Hardware Architecture Overview

Since an area and energy-efficient microarchitecture is crucial to make co-integration of sPIN accelerator and NIC feasible, we leverage the parallel ultra low power (PULP) platform for this estimation [27, 28]. PULP is a clustered many-core architecture that employs fully programmable 32 bit RISC-V cores [29] as main processing elements. The PULP architecture is geared towards area and energy-efficiency, and hence data movement is controlled in software using DMA transfers between local scratchpad memories (SPMs) in order to minimize communication-related overheads. Apart from being more efficient than designs with hardware-managed caches [28], this approach ensures tight control over the compute and data movement schedule, leading to predictable execution patterns with low variance. Hence, PULP is an ideal architectural template for sPIN, and the fact that the project is completely open-source facilitates the analysis and dissemination of the results.

Fig. 9a shows a high-level overview of the proposed accelerator architecture, which is based on a PULP multicluster [27] that has been modified to meet the requirements of this application (the central elements are highlighted with a blue border). The analyzed configuration comprises four clusters with eight cores each. To stay above the memory requirements, the architecture contains 12 MiB of memory distributed over two hierarchy levels with 16-64 KiB L1 SPM banks per cluster and 2-4 MiB L2 SPM banks on the top-level. The L1 SPM is private to each cluster and split into twice as many banks as cores to keep contention low (typically <10%). Cores can

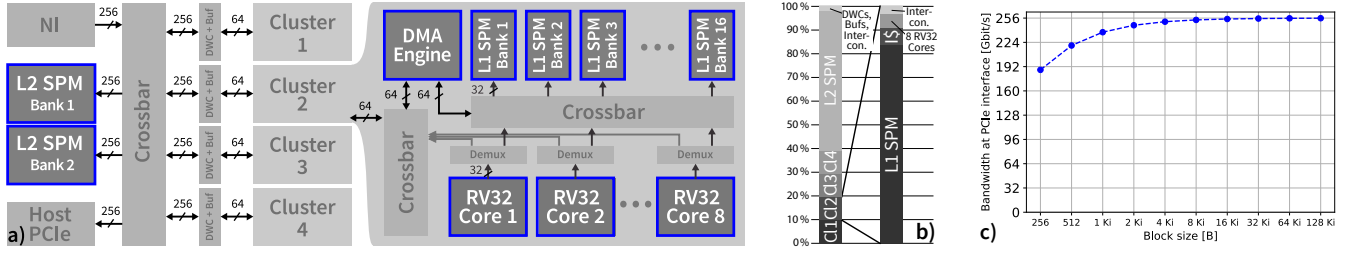


Figure 9: a) Proposed hardware architecture of the SPIN accelerator. Single-headed arrows indicate half-duplex, and double-headed arrows full-duplex bandwidth. b) Area breakdown of the accelerator. c) Bandwidth in function of block size.

read and write to L1 SPM within a single cycle and use it as low-latency shared memory and for fine-grained synchronization. Each cluster contains a multi-channel DMA for efficient data movement.

4.2 Throughput Considerations

The discussed configuration runs at up to 1 GHz in the target technology, and hence the raw compute throughput amounts to 32 Gop/s, fulfilling the requirement of 2 Gop/s and providing ample headroom for cases where more compute power is needed instantaneously (e.g., bursts of complex datatypes). Further, the memories and system interconnects have been sized to be 256 bit wide to sustain a line rate of 200 Gbit/s.

New packets enter the accelerator over a 256 bit wide input port on the network side, and are first placed in the L2 SPM. The cluster-private DMAs then transfer the data to the local L1 SPMs. After processing, the results are directly transferred from the L1 SPMs to the 256 bit output port on the PCIe side. Since the L2 needs to sustain a bidirectional bandwidth of $2 \cdot 256$ Gbit, it has been split into two banks with separate ports into the system interconnect. Each cluster processes, on average, one fourth of the incoming data, and hence each DMA can transfer 64 bit/cycle in each direction.

4.3 Cycle Accurate Simulations

The cycle-accurate testbed is comprised of synthesizable SystemVerilog models that are simulated with Mentor QuestaSim. The NIC/P-PCIe interfaces are abstracted as a bus-attached memory region and a FIFO, respectively.

4.3.1 Bandwidth. To measure the effective bandwidth of memories, interconnect, and DMA engines, we created a benchmark where cores continuously transfer data blocks from L2 to the local L1 and then to the host PCIe using DMA bursts. The block size is varied from 256 B to 128 KiB. As shown in Fig. 9c), a throughput of 192 Gbit/s can be reached for blocks of 256 B, and all higher block sizes are above the line rate.

4.3.2 Microkernels. To study the performance of datatype processing on PULP, we benchmark the RW-CP handlers on a 1 MiB message with a vector datatype, varying the block size. Fig. 10 shows the throughput achieved by simulating DDT processing on PULP (cycle-accurate) and compares it with the ones of a ARM-based simulation (SST+gem5, see Sec. 5.1).

The benchmark creates dummy packets and HERs in the L2 memory and statically assigns the HERs to the cores. To emulate the blocked-RR scheduling strategy used by RW-CP, we assign consecutive blocks of 4 packets (2 KiB/packet) to each core. We report the

achieved throughput based on the maximum time needed by a core to process all the assigned packets. We keep the dataloops (i.e., the datatype description) in L2 and move the checkpoints into the L1 of the cluster where the handlers using them are run.

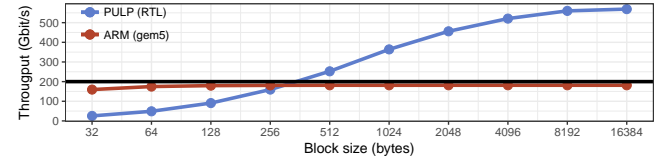


Figure 10: DDT processing throughput on ARM and PULP.

The PULP-based implementation is slower than the ARM-based one for small block sizes (i.e., < 256 B): in these cases the handlers run longer because of the higher number of contiguous blocks per packet, making more accesses to L2, thus increasing memory contention. However, we have also to take into account that the gem5-based simulation may not model memory contention properly, or at least not as good as the cycle accurate simulation we use for PULP. The impact of L2 contention is visible also in Fig. 11, that shows the instructions-per-cycle (IPC) of the RW-CP handlers on PULP: small block sizes lead to lower IPCs due to the more frequent L2 accesses. The PULP-based DDT processing achieves line rate for block sizes larger than 256 bytes. After that, line rate is exceeded because the experiment is not capped by the network bandwidth (the packets are preloaded in L2). We reserve a more in-depth evaluation and optimization (e.g., transparently moving dataloops to L1) of a SPIN implementation on PULP for future work.

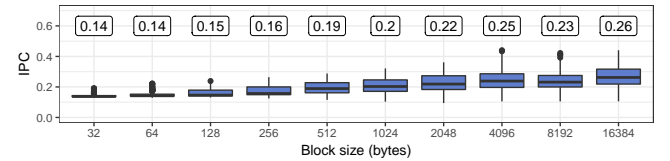


Figure 11: RW-CP Instructions per Cycle (IPC) on PULP. The median IPC for each block size is annotated on the top.

4.4 Circuit Complexity and Power Estimations

We synthesized the processor in GlobalFoundries' 22 nm fully depleted silicon on insulator (FDSOI) technology using Synopsys DesignCompiler, and were able to close the timing of the system at 1 GHz. Including memories, the entire accelerator has a complexity of approximately 100 MGE¹. Fig. 9b) shows the area breakdown of the entire accelerator (left) and of one processing cluster (right). The

¹ 1 gate equivalent (GE) equals $0.199 \mu\text{m}^2$, the area of two-input NAND gate in 22 nm.

four clusters together account for ca. 39% of the total accelerator area, and the remaining part is mainly dominated by the 8 MiB of L2 SPM (59%). The system interconnect, DWCs, and buffers only amount to around 2%. Within one cluster, the 1 MiB L1 SPM accounts for 84% of the area, the rest is taken by the shared instruction cache (7%), the eight RISC-V cores (6%), and the DMA engine and interconnects (3%). Assuming a conservative layout density of 85%, 100 MGE equal 23.5 mm^2 of silicon area.

To put this in perspective, we compare the silicon area of the proposed sPIN accelerator with the compute subsystem of the BlueField SmartNIC system-on-chip (SoC) from Mellanox [30]. These devices contain two 100 Gbit Ethernet ports, a Gen4 16× PCIe port and an additional ARM subsystem with up to 16 A72 64 bit cores with 1 MiB shared L2 cache per 2 cores, and 6 MiB shared L3 last-level cache. From [31, 32] it can be inferred that one A72 dual-core tile occupies around 5.6 mm^2 in 22 nm technology, and hence a full 16 core configuration amounts to around 51 mm^2 . Hence, with an overall complexity of 23.5 mm^2 , we observe that the analyzed parameterization of the proposed accelerator only occupies about 45% of the area budget allocated for the processing subsystem in this related commercial device. Note that the presented architecture is modular and could be re-parameterized based on the technology node, available silicon area and application needs. E.g., with a similar area budget as on the BlueField SoC, we could double the amount of clusters and memory to 64 RISC-V cores and 18 MiB.

In terms of power consumption, we estimate (using a back-annotated gate-level power simulation) that this design requires around 6 W under full load (not including I/O and PHY power), which is comparable to the typical power consumption that has been measured for PCIe NIC cards (4.6–21.2 W) [33].

4.5 Discussion

The PULP platform well matches the sPIN abstract machine, making it a first-class candidate for a sPIN implementation. The main research directions we plan to explore in this context are: (1) Extend the sPIN programming model in order to let the user specify which data should be moved to L1. In fact, as discussed in Sec. 4.3.2, L2 contention can quickly become an issue for performance. (2) Design a sPIN runtime running on PULP. The runtime is in charge to manage the cores/clusters, assigning new HERs to execute to the idle ones, and serve the commands issued by the handlers (e.g., DMA read/writes, new network operations). (3) Deeply evaluate further use cases in order to validate our design choices.

5 EVALUATION

We evaluate the effects of datatypes processing offload using an extensive set of simulations on a modified version of Cray Slingshot Simulator. We now describe the simulation setup, then we discuss the microbenchmarks that are used to study the performance and NIC resource usage for DDT offloading solutions. Finally, we show the performance improvements that can be achieved on full HPC applications. Hardware implementation aspects of sPIN will be discussed in Sec. 4.

5.1 Simulation Setup

To analyze the effects of integrating sPIN in next-generation networks, we extend the Cray Slingshot Simulator, which models a

200 Gib/s NIC (see Fig. 1) in Sandia Structural Simulation Toolkit (SST) [34], adding packet processing capabilities by implementing sPIN. We configure the network simulator to send 2 KiB of payload data. We combine the network simulator with gem5 [35], that accurately simulates ARM-based architectures [36], to simulate the handlers execution. The HPUs are modeled as 64-bit A15 processors [37]. We associate each NIC with a gem5 system, configured with 32 Cortex A15 clocked at 800 MHz (unless otherwise specified). The NIC memory is simulated with the gem5's SimpleMemory module, that can support k-cycles latency memory accesses (we use $k = 1$ in this paper) with a bandwidth of 50 GiB/s and a number of channels equal to two times the number of HPUs. The host-NIC interface is modeled as a x32 PCIe Gen4: the simulation accounts for PCIe packets overheads and a 128b/130b encoding scheme. The SST-gem5 integration follows the same approach adopted by Hoefler et al. to simulate sPIN handlers in LogGOPSim [38].

The host-based unpack function is profiled by running the MPI-Types unpack function (i.e., `MPIT_Type_memcpy`) on a Intel i7-4770 CPU @3.4GHz equipped with 32 GiB of DRAM. Each measure is taken until the 99% CI is within the 10% of the reported median. For RW-CP we set $\epsilon = 0.2$. (see Sec. 3.2.4), so to keep the scheduling overhead less than 20 % of the message processing time.

5.2 Microbenchmarks

The microbenchmarks presented in this section are based on the offloading of an MPI vector datatype. We observe similar results for other MPI derived datatypes but omit them due to space limitations.

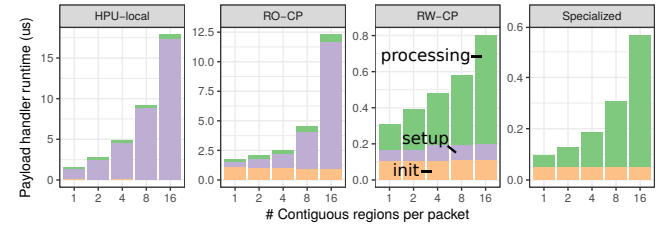


Figure 12: Payload handlers execution breakdown for different strategies and block sizes.

Unpack Throughput. Fig. 8 shows the receive throughput for a 4 MiB message described with a vector datatype, varying the block sizes. This value is computed considering the time from when the *ready-to-receive* message is sent to the sender (i.e., to avoid that data message arrives unexpectedly) to when the last byte of data is copied into its final position in the receiver memory.

For small block sizes, the offloaded approaches lose their effectiveness, becoming more expensive than the host-based unpack for 4 byte blocks. This behavior is explained by Fig. 12, that shows a breakdown of the handlers runtime for small block sizes. We report the handlers performance as function of γ , i.e., the number of contiguous regions per packet, varying it from 1 (i.e., block size of 2048 B) to 16 (i.e., block size of 128 B).

The HPU-local handler runtime is always dominated by the *setup* time (including the MPITypes catch-up phase). RO-CP spends more time in the *init* phase, where the checkpoint gets copied, and is also involved in long catch-up phases (e.g., 87% of the total time for $\gamma = 16$). RW-CP is only a factor of two slower than the specialized handler, explaining the high throughput reached in Fig. 8.

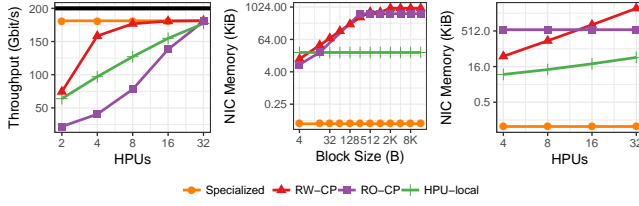


Figure 13: From left to right: Receive throughput scalability; NIC Memory occupancy as function of the block size; NIC Memory occupancy as function of the number of HPUs.

Scalability. Fig. 13a shows the receive throughput for different numbers of HPUs, fixing the block size to 2 KiB (i.e., $\gamma = 1$). The specialized handler reaches line rate already with two HPUs, while the others are limited by the respective overheads (i.e., scheduling for RW-CP, catch-up for HPU-local, copy and catch-up for RO-CP).

Fig. 13b shows the NIC memory occupancy for different block sizes, fixing the number of HPUs to 16. While the HPU-local and specialized occupancy remains fixed, the checkpointed variants adjust the checkpoint interval to keep their scheduling overhead less than ϵ , as described in Sec. 3.2.4. In particular, the larger the block size, the faster the message processing time, the smaller will be the checkpoint interval (leading to higher NIC memory occupancy).

Fig. 13c shows the NIC memory occupancy for different number of HPUs. The memory resources required by the HPU-local strategy increase with the number of HPUs because the segment data structure is replicated on each HPU. For RW-CP, by increasing the number of HPUs we make the DDT processing faster, leading the checkpoint interval selection heuristic to increase the number of checkpoints, thus the higher NIC memory occupancy.

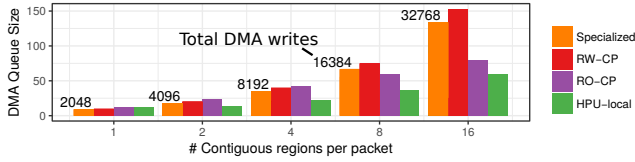


Figure 14: Maximum DMA write requests queue occupancy over the entire message processing time.

PCIe Traffic. In this microbenchmark we study the PCIe traffic generated by different handlers. Fig. 14 shows the maximum DMA queue occupancy that has been reached during the message processing, for different values of γ (x-axis) and different handlers (bars). Each group of bars is annotated with the total number of DMA writes that are issued for that specific value of γ . The number of HPUs is fixed to 16. In all the cases, the PCIe request buffer is kept under 160 requests, meaning that PCIe was not a bottleneck.

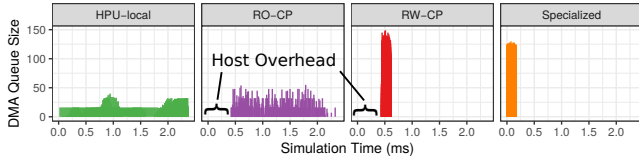


Figure 15: DMA write requests queue over time for $\gamma = 16$ and different datatype processing strategies.

Fig. 15 shows the DMA FIFO queue size over time for handlers processing a message with $\gamma = 16$ (i.e., 128 B block sizes). The HPU-local and RO-CP strategy have the slowest handlers, which translates

to a small number of DMA requests issued per second, explaining a low DMA queue occupancy. The RW-CP and specialized strategies have higher peak occupancy due to their faster handlers. The figure also shows the time needed by the host to create the checkpoints and copy them to NIC memory (i.e., *host overhead*).

5.3 Real Applications DDTs

We analyze a set of datatypes used in real applications and for different input parameters. The selected applications cover different domains such as atmospheric sciences, quantum chromodynamics, molecular dynamics, material science, geophysical science, and fluid dynamics [8]. The selected applications are:

- **COMB** [39]: a communication performance benchmarking tool for common communication patterns on HPC platforms. The tool represents exchange of data stored in n-dimensional arrays that are distributed across one or more dimensions.
- **FFT2D** [9]: performs a Fast Fourier Transform (FFT) for a 2D distributed matrix by row-column algorithm which composes 2D transform from two one-dimensional FFT applied to rows and then to columns. Such algorithm requires transposing the matrix which can be expressed as a non-contiguous data access.
- **LAMMPS** [40]: a molecular dynamics simulator for materials modeling. The application exchanges the physical properties of moving particles using index datatypes. Depending on simulation settings, the particles can have different number of properties, therefore, we create two tests: *LAMMPS_full* and *LAMMPS*.
- **MILC** [41]: a large scale numerical simulation for quantum chromodynamics. We use the lattice quantum chromodynamics which performs halo-exchange of 4D regular grid of points.
- **NAS** [15]: a fluid dynamics simulation system solving Navier-Stokes equations. It consists of two micro-applications: *NAS_MG* and *NAS_LU*. *NAS_MG* communicates the faces of a 3D array, and *NAS_LU* solves a three-dimensional system of equations.
- **SPECFEM3D** [42]: simulates seismic wave propagation problems using Finite Element Method. It uses indexed datatypes for exchanging mesh grid points with neighboring processes and exhibits two different exchange patterns (*FEM3D_loc,cm*), which differ in the amount of data communicated per index.
- **SW4LITE** [43]: a performance testing library which solves seismic wave equations in Cartesian coordinates for 3-D seismic modeling. It uses different datatypes for exchanging data with neighboring processes: we distinguish between exchanges along x and y directions, and define two tests: *sw4_x* and *sw4_y*.
- **WRF** [44]: a numerical weather prediction system. It represents the space as 3 dimensional Cartesian grid, and performs halo exchanges of structs of subarray datatypes. We define two tests depending on the exchange direction: *wrf_x* and *wrf_y*.

Figure 16 shows the speedup of the RW-CP and specialized handlers w.r.t. the host-based unpack for different datatypes and message sizes employed by the above described applications. The host-based unpacking receives the full message and then unpacks it with MPI types. The benchmark is executed with cold caches to model the scenario where the message has just been copied from the NIC to main memory (we assume no direct cache placement of the DMA writes). We compare the achieved speedups with a Portals 4-based unpacking solution. This solution uses input/output vectors (iovecs) and assumes the NIC being able to store a number v of iovec entries:

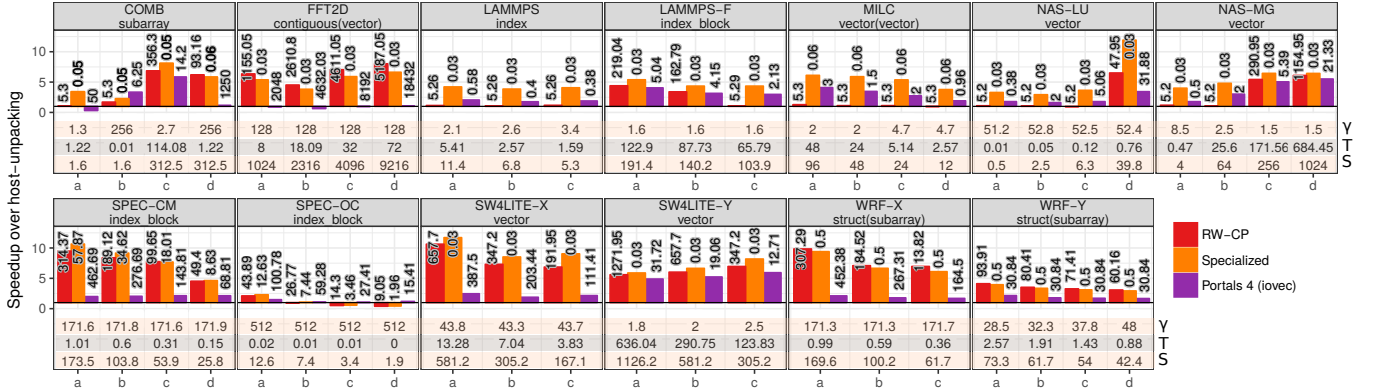


Figure 16: Message processing time speedup for different DDT kernels. For each input, we report γ : average number of blocks per packet; T: the baseline, that is the message processing time for the host-based unpacking (ms); S: the message size (KiB). The bars are annotated with the amount of data (KiB) moved to the NIC to support the unpack.

Every received v blocks, the NIC issues a PCIe read (modeled with a 500ns latency [45, 46]) from main memory to get the next v iovecs. We use $v = 32$, that is the maximum number of scatter-gather entries for a Mellanox ConnectX-3 card [2] (no Portals 4 implementation is publicly available at the time of writing). This model assumes in-order packet arrival.

For each experiment, we report the average number of blocks per packet (γ), the message processing time of the host-based solution (T), and the message size (S). The bars are annotated with the size of data moved to the NIC in order to offload DDT processing: RW-CP needs to copy the MPI types dataloops describing the datatype and the checkpoints (see Sec. 3.2.4); the specialized handler always require the minimum amount of space (e.g., the list of offsets and block sizes for the index datatype); the Portals 4 solution needs to move the entire iovec list, which size is linear in the number of contiguous regions identified by the datatype.

RW-CP and native can reach up to 12x speedup over the host-based unpacking. The offloaded datatype processing strategies do not introduce any speedup in the cases where the message size is small (i.e., the first two COMB experiments send messages fitting in one packet) or if the number of blocks per packet is large (e.g., SPEC-OC has $\gamma = 512$ blocks per packet). In the first case, the datatype processing cannot exploit the NIC parallelism and the datatype processing is only delayed by the handler latency. In the second case, the message processing time increases because of: (1) the increased handler runtime, that is linear in the number of contiguous regions; (2) the inefficient utilization of the PCIe bus (i.e., with $\gamma = 512$, the handlers issue 512 DMA writes of 4 bytes).

Memory Transfers. Host-based message unpacking requires the NIC to first write the received (packed) message in a memory buffer so the CPU can unpack it. During the unpack, the CPU needs to access the entire packed data and all the parts of the receive buffer where the message has to be copied to. Instead, by offloading the datatype processing task, the only memory accesses that are needed are the ones that the NIC does to write the data directly in the receive buffer. In Fig. 17 we show the total data volume that is moved to and from the main memory to receive and unpack a message for RW-CP and host-based unpacking.

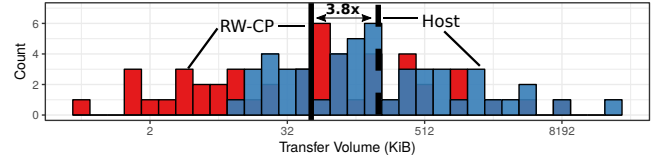


Figure 17: Histogram of the data volumes moved to/from main memory by RW-CP and host-based unpacking for the experiments of Fig. 16. The vertical lines represent the geometric mean of the moved data volumes for RW-CP (continuous line) and host-based unpacking (dashed line).

We report how many experiments of Fig. 16 (y-axis) needed to move a specific amount of data (x-axis) for completing the message unpacking. For RW-CP, the data volume written to main memory always corresponds to the message size. For the host-based unpack, the data volume is the message size (moved from the NIC to the main memory) plus the data transferred between the last-level cache and the main memory during the unpack (measured as number of last-level cache misses times the cache line size). The reported geometric mean shows that RW-CP moves 3.8x less data than the host-based unpack.

Amortizing Checkpointing Cost. The RW-CP strategy requires the application to create checkpoints before starting to receive the data to unpack. But, *how long does it take to produce and copy these checkpoints to the NIC?* We answer this question with the data shown in Fig. 18. Instead of reporting an absolute number, we report for each application/input combination of Fig. 16 the number of times a datatype should be used in order to amortize the checkpoint creating cost. In the 75% of the cases, the speedup introduced by RW-CP pays off after < 4 reuses of the same datatype. It is worth noting that the checkpoints are independent from the receive buffer (i.e., they are

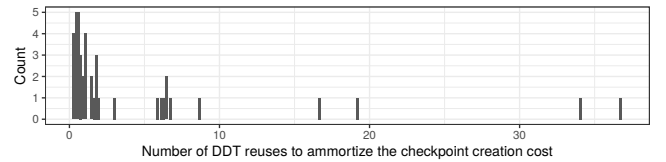


Figure 18: Number of times a datatype needs to be reused to amortize the checkpoint creation overhead for RW-CP.

used to compute offsets), hence the checkpoint creation cost is paid only once per datatype. With *iovecs*, instead, each *iovec* entry needs to have the virtual address where the block starts, hence a *iovec* list needs to be created every time the receive buffer changes.

5.4 Application Scalability

To study the effects of offloading datatype processing we benchmark the full FFT2D application at large scales. The application partitions the input matrix by rows and performs two 1D-FFT operations. The second one is applied after the matrix is transposed with a `MPI_Alltoall` operation. After the second 1D-FFT finishes, the matrix is transposed back to the original layout. We use the same approach of Hoefler et al. [9], that avoids the manual matrix transposition by encoding this operation as MPI Datatypes.

We simulate the effect of offloading the datatype processing (hence the matrix transposition) to sPIN at large scales. In particular, given a communicator size, we simulate the unpack cost of the receive datatype with the SST and measure the 1D-FFT time for the different workloads (see Sec. 5.1 for the detailed configuration). We use these two parameters to build a GOAL [47] trace for FFT2D at different scales. We then run the trace with LogGOPSim, that is configured to model next-generation networks [14].

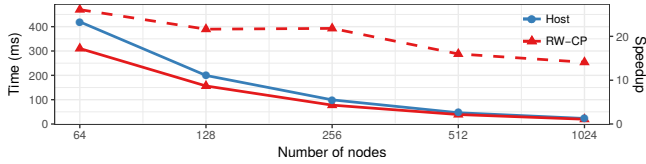


Figure 19: FFT2D strong scaling: runtime (continuous) and speedup (% , dashed) of RW-CP over host-based unpacking.

Fig. 19 shows the FFT2D strong scaling for a matrix $n \cdot n$ with $n = 20,480$. At $P = 64$ the runtime of each node is split in $\sim 60\%$ computation and $\sim 40\%$ communication: offloading datatype processing accelerates the application up to 26% of the host-based unpack version (i.e., MPI Types). Increasing the number of nodes, the unpack overhead shrinks, reducing the effects of optimizing it.

6 RELATED WORK

We discussed the various solutions to support non-contiguous memory transfers in Sec. 2.2. Several works have been focusing on optimizing MPI datatypes with different approaches: Traff et al. [48] show that some complex derived datatypes can be transformed into simpler ones, improving the packing and unpacking performance with a more compact representation. Gropp et al. [21] provide a classification of the MPI derived datatypes based on their memory access patterns, discussing how they can be efficiently implemented or automatically optimized [22]. Both approaches are orthogonal to this work because they propose optimizations that can be applied before offloading and can be integrated in the offloaded handlers.

Offloading DDT processing to GPU systems has been discussed by Wang et al. [13]. However, unpacking data on GPUs still requires the data to be fully received on the GPU memory before the unpack can start. In this work, we discuss how datatype processing can be performed as the stream of data arrives, truly implementing zero-copy non-contiguous memory transfers.

Non-contiguous memory transfers can be accelerated by compiling DDTs pack/unpack functions at runtime [11, 49]. However, the main optimization of this approach is to choose the best data copying strategy for x86 architectures [50]. The same cannot be applied to NICs, where the only way to move data to the host is by issuing DMA writes to it. The performance we expect from runtime-compilation is the same of the specialized handlers shown in this work. Our interpretation-based offload approach (i.e., RW-CP) has lower startup cost, since there is no compilation step necessary, and shows performances similar to the specialized handlers.

The idea of triggering handlers in response to incoming data has been explored with Active Messages [51, 52] for message-passing and with Active Accesses [53] for one-sided operations. While these solutions can be used to trigger datatype unpacking routines, they only express handlers as function of the received message (i.e., no streaming processing) and they are run on the host CPU. In sPIN the handlers are defined on a per-packet basis and run directly on the NIC, enabling datatype processing on the fly. Di Girolamo et al. [6] propose an abstract machine model to express offloaded communication/computation schedules: DDT processing can be modeled with such schedules (i.e., triggered puts targeting the local node to scatter the data). However, also in this case the processing can only start after the full message has been received and it requires a number of NIC resources linear in the number of contiguous blocks.

7 CONCLUSIONS

We presented different solutions to accelerate non-contiguous memory transfers exploiting next-generation network accelerators like sPIN. We identify what are the challenges of offloading MPI derived datatypes, the most expressive interface to describe non-contiguous memory regions, and how sPIN can be extended to efficiently support on-the-fly datatype processing. To back our simulations studies, we outline a real hardware implementation of sPIN. We then provide an extensive evaluation showing how communications can benefit from network-accelerated datatype processing.

Acknowledgements

This project has received funding from the European Research Council (ERC) under the European Union’s Horizon 2020 programme (grant agreements: DAPP, No. 678880; OPRECOMP, No. 732631). Jakub Beránek has been supported by the European Science Foundation through the “Science without borders” project, reg. nr. CZ.02.2.69/0.0./0.0./16_027/0008463 within the Operational Programme Research, Development and Education. We thank David Hewson for the insightful discussions and Cray Inc. for supporting this project.

REFERENCES

- [1] T. Shanley. 2003. *Infiniband Network Architecture*. Addison-Wesley Professional.
- [2] 2019. Mellanox Technologies. <http://www.mellanox.com/>. (2019).
- [3] B. Alverson, et al. 2012. Cray XC series network. *Cray Inc., White Paper WP-Aries01-1112* (2012).
- [4] B. W. Barrett, et al. 2018. The Portals 4.2 Network Programming Interface. *Sandia National Laboratories, November 2012, Technical Report SAND2012-10087* (2018).
- [5] T. Schneider, et al. 2013. Protocols for Fully Offloaded Collective Operations on Accelerated Network Adapters. In *Parallel Processing (ICPP), 2013 42nd International Conference on*. 593–602.
- [6] S. Di Girolamo, et al. 2016. Exploiting Offload Enabled Network Interfaces. *IEEE MICRO* 36, 4 (Jul. 2016).

- [7] T. Schneider, R. Gerstenberger, and T. Hoefler. 2012. Micro-Applications for Communication Data Access Patterns and MPI Datatypes. In *Recent Advances in the Message Passing Interface - Proceedings of the 19th European MPI Users' Group Meeting, EuroMPI 2012, 2012.*, Vol. 7490. Springer, 121–131.
- [8] T. Schneider, R. Gerstenberger, and T. Hoefler. 2014. Application-oriented ping-pong benchmarking: how to assess the real communication overheads. *Journal of Computing* 96, 4 (Apr. 2014), 279–292.
- [9] T. Hoefler and S. Gottlieb. 2010. Parallel Zero-Copy Algorithms for Fast Fourier Transform and Conjugate Gradient using MPI Datatypes. In *Recent Advances in the Message Passing Interface (EuroMPI'10)*, Vol. LNCS 6305. Springer, 132–141.
- [10] W. Gropp, et al. 2011. Performance Expectations and Guidelines for MPI Derived Datatypes. In *Recent Advances in the Message Passing Interface (EuroMPI'11)*, Vol. 6960. Springer, 150–159.
- [11] T. Schneider, F. Kjolstad, and T. Hoefler. 2013. MPI Datatype Processing using Runtime Compilation. In *Proceedings of the 20th European MPI Users' Group Meeting*. ACM, 19–24.
- [12] G. Santhanaraman, J. Wu, and D. K. Panda. 2004. Zero-copy MPI derived datatype communication over InfiniBand. In *European Parallel Virtual Machine/Message Passing Interface Users' Group Meeting*. Springer, 47–56.
- [13] H. Wang, et al. 2011. Optimized non-contiguous MPI datatype communication for GPU clusters: Design, implementation and evaluation with MVAPICH2. In *2011 IEEE International Conference on Cluster Computing*. IEEE, 308–316.
- [14] T. Hoefler, et al. 2017. sPIN: High-performance streaming Processing in the Network. In *Proceedings of the International Conference for High Performance Computing, Networking, Storage and Analysis (SC17)*.
- [15] R. F. Van der Wijngaart and P. Wong. 2002. NAS parallel benchmarks version 2.4. (2002).
- [16] J. Nieplocha, et al. 2006. High performance remote memory access communication: The ARMCI approach. *The International Journal of High Performance Computing Applications* 20, 2 (2006), 233–253.
- [17] B. Chapman, et al. 2010. Introducing OpenSHMEM: SHMEM for the PGAS community. In *Proceedings of the Fourth Conference on Partitioned Global Address Space Programming Model*. ACM, 2.
- [18] J. Mellor-Crummey, et al. 2009. A new vision for Coarray Fortran. In *Proceedings of the Third Conference on Partitioned Global Address Space Programming Models*. ACM, 5.
- [19] T. El-Ghazawi and L. Smith. 2006. UPC: unified parallel C. In *Proceedings of the 2006 ACM/IEEE conference on Supercomputing*. ACM, 27.
- [20] Message Passing Interface Forum. 2012. MPI: A Message-Passing Interface Standard Version 3.0. (09 2012). Chapter author for Collective Communication, Process Topologies, and One Sided Communications.
- [21] W. Gropp, E. Lusk, and D. Swider. 1999. Improving the performance of MPI derived datatypes. In *Proceedings of the Third MPI Developer's and User's Conference*. MPI Software Technology Press, 25–30.
- [22] S. Byna, et al. 2006. Automatic memory optimizations for improving MPI derived datatype performance. In *European Parallel Virtual Machine/Message Passing Interface Users' Group Meeting*. Springer, 238–246.
- [23] N. Tanabe and H. Nakajo. 2008. Introduction to acceleration for MPI derived datatypes using an enhancer of memory and network. In *European Parallel Virtual Machine/Message Passing Interface Users' Group Meeting*. Springer, 324–325.
- [24] J. L. Träff. 2014. Optimal MPI Datatype Normalization for Vector and Index-block Types. In *Proceedings of the 21st European MPI Users' Group Meeting (EuroMPI/ASIA '14)*. ACM, New York, NY, USA, Article 33, 6 pages. DOI: <http://dx.doi.org/10.1145/2642769.2642771>
- [25] R. Ross, et al. 2009. Processing MPI datatypes outside MPI. In *European Parallel Virtual Machine/Message Passing Interface Users' Group Meeting*. Springer, 42–53.
- [26] R. Ross, N. Miller, and W. D. Gropp. 2003. Implementing fast and reusable datatype processing. In *European Parallel Virtual Machine/Message Passing Interface Users' Group Meeting*. Springer, 404–413.
- [27] A. Kurth, et al. 2017. HERO: Heterogeneous embedded research platform for exploring RISC-V manycore accelerators on FPGA. *arXiv preprint arXiv:1712.06497* (2017).
- [28] D. Rossi, et al. 2017. Energy-Efficient Near-Threshold Parallel Computing: The PULPv2 Cluster. *IEEE Micro* 37, 5 (Sep. 2017), 20–31.
- [29] M. Gautschi, et al. 2017. Near-Threshold RISC-V Core With DSP Extensions for Scalable IoT Endpoint Devices. *IEEE Transactions on Very Large Scale Integration (VLSI) Systems* 25, 10 (Oct 2017), 2700–2713. DOI: <http://dx.doi.org/10.1109/TVLSI.2017.2654506>
- [30] Mellanox Technologies. 2019. Mellanox BlueField SmartNIC. http://www.mellanox.com/related-docs/prod_adapter_cards/PB_BlueField_Smart_NIC.pdf. (2019). Online; accessed 05. April 2019.
- [31] H. T. Mair, et al. 2016. 4.3 A 20nm 2.5GHz ultra-low-power tri-cluster CPU subsystem with adaptive power allocation for optimal mobile SoC performance. In *IEEE International Solid-State Circuits Conference (ISSCC)*. 76–77.
- [32] J. Pyo, et al. 2015. 23.1 20nm high-K metal-gate heterogeneous 64b quad-core CPUs and hexa-core GPU for high-performance and energy-efficient mobile application processor. In *2015 IEEE International Solid-State Circuits Conference - (ISSCC) Digest of Technical Papers*. 1–3.
- [33] R. Sohan, et al. 2010. Characterizing 10 Gbps network interface energy consumption. In *IEEE Local Computer Network Conference*. 268–271.
- [34] C. L. Janssen, et al. 2010. A simulator for large-scale parallel computer architectures. *International Journal of Distributed Systems and Technologies (IJDSST)* 1, 2 (2010), 57–73.
- [35] Nathan Binkert, et al. 2011. The gem5 simulator. *ACM SIGARCH Computer Architecture News* 39, 2 (2011), 1–7.
- [36] F. A. Endo, D. Couroussé, and H. Charles. 2014. Micro-architectural simulation of in-order and out-of-order arm microprocessors with gem5. In *2014 International Conference on Embedded Computer Systems: Architectures, Modeling, and Simulation (SAMOS XIV)*. IEEE, 266–273.
- [37] A. Tousi and C. Zhu. 2017. Arm Research Starter Kit: System Modeling using gem5. (2017).
- [38] T. Hoefler, T. Schneider, and A. Lumsdaine. 2010. LogGOPSim - Simulating Large-Scale Applications in the LogGOPS Model. In *Proceedings of the 19th ACM International Symposium on High Performance Distributed Computing*. ACM, 597–604.
- [39] Lawrence Livermore National Laboratory. 2018. Comb is a communication performance benchmarking tool. (2018). <https://github.com/LLNL/Comb>
- [40] S. Plimpton. 1995. Fast Parallel Algorithms for Short-range Molecular Dynamics. *J. Comput. Phys.* 117, 1 (March 1995), 1–19. DOI: <http://dx.doi.org/10.1006/jcph.1995.1039>
- [41] C. Bernard, et al. 1991. Studying quarks and gluons on MIMD parallel computers. *The International Journal of Supercomputing Applications* 5, 4 (1991), 61–70.
- [42] L. Carrington, et al. 2008. High-frequency Simulations of Global Seismic Wave Propagation Using SPECfem3D GLOBE on 62K Processors. In *Proceedings of the 2008 ACM/IEEE Conference on Supercomputing (SC '08)*. IEEE Press, Piscataway, NJ, USA, Article 60, 11 pages. <http://dl.acm.org/citation.cfm?id=1413370.1413432>
- [43] B. Sjogreen. 2018. SW4 final report for iCOE. Technical Report. Lawrence Livermore National Lab.(LLNL), Livermore, CA (United States).
- [44] W. C. Skamarock and J. B. Klemp. 2008. A Time-split Nonhydrostatic Atmospheric Model for Weather Research and Forecasting Applications. *J. Comput. Phys.* 227, 7 (March 2008), 3465–3485. DOI: <http://dx.doi.org/10.1016/j.jcp.2007.01.037>
- [45] R. Neugebauer, et al. 2018. Understanding PCIe performance for end host networking. In *Proceedings of the 2018 Conference of the ACM Special Interest Group on Data Communication*. ACM, 327–341.
- [46] M. Martinasso, et al. 2016. A PCIe Congestion-Aware Performance Model for Densely Populated Accelerator Servers. In *Proceedings of the International Conference for High Performance Computing, Networking, Storage and Analysis (SC16)*. IEEE Press, 63:1–63:11.
- [47] T. Hoefler, C. Siebert, and A. Lumsdaine. 2009. Group Operation Assembly Language - A Flexible Way to Express Collective Communication, In ICPP-2009 - The 38th International Conference on Parallel Processing. (Sep. 2009).
- [48] J. L. Träff, et al. 1999. Flattening on the Fly: efficient handling of MPI derived datatypes. In *Recent Advances in Parallel Virtual Machine and Message Passing Interface*, Jack Dongarra, Emilio Luque, and Tomàs Margalef (Eds.). Springer Berlin Heidelberg, Berlin, Heidelberg, 109–116.
- [49] T. Prabhu and W. Gropp. 2015. DAME: A runtime-compiled engine for derived datatypes. In *Proceedings of the 22nd European MPI Users' Group Meeting*. ACM, 4.
- [50] T. Schneider, R. Gerstenberger, and T. Hoefler. 2013. Compiler optimizations for non-contiguous remote data movement. In *International Workshop on Languages and Compilers for Parallel Computing*. Springer, 307–321.
- [51] TV Eicken, et al. 1992. Active messages: a mechanism for integrated communication and computation. In *[1992] Proceedings the 19th Annual International Symposium on Computer Architecture*. IEEE, 256–266.
- [52] M. Besta and T. Hoefler. 2015. Accelerating Irregular Computations with Hardware Transactional Memory and Active Messages. In *Proceedings of the 24th Symposium on High-Performance Parallel and Distributed Computing (HPDC'15)*. ACM, 161–172.
- [53] M. Besta and T. Hoefler. 2015. Active Access: A Mechanism for High-Performance Distributed Data-Centric Computations. In *Proceedings of the 29th International Conference on Supercomputing (ICS'15)*. ACM, 155–164.